Available online at www.sciencedirect.com

ScienceDirect

IFAC PapersOnline CONFERENCE PAPER ARCHIVE

IFAC PapersOnLine 53-5 (2020) 464–469

An Application of Affective Computing on Mental Disorders: A Resting State fNIRS Study ⋆

Chunyun Wu, Jieqiong Sun, Tao Wang, Chengjian Zhao, Shuzhen Zheng, Chang Lei, Hong Peng *

*Gansu Provincial Key Laboratory of Wearable Computing, School of Information Science and Engineering, Lanzhou University, Lanzhou 730000, China (e-mail: {wuchy18, sunjq18, wangtao2018, zhaochj18, zhengshzh19, leich19, pengh}@lzu.edu.cn). * Corresponding author*

Abstract: Affective computing is important for making computers smarter. When emotion can be quantified, machines can understand it. This study aims to apply affective computing to mental disorders, and to classify healthy people and mentally illnesses. For this purpose, 85 subjects, including major depressive disorder patients, schizophrenia patients, and health control people were recruited to participate in resting state functional near infrared spectroscopy (fNIRS) experiment. We measured the changes in oxygenated blood concentration in the prefrontal cortex (PFC). We then used three types of correlation analysis methods to construct the functional connectivity matrices: Pearson correlation analysis (CORR), amplitude squared coherence coefficient (COH), and phase locking value (PLV). We performed the small-world model and centrality analysis based on these matrices. The results demonstrated the existence of a small-world model in both patients and healthy people's brain networks. Furthermore, features such as the characteristic path length and betweenness centrality extracted from the functional connectivity matrix are helpful for classifying patients and healthy people, thus providing a method for detecting and identifying mental disorders.

Keywords: Affective Computing, fNIRS, Brain Network, Mental Disorder

1. INTRODUCTION

Affective computing aims to improve intelligence in computers by giving them the ability to recognize, understand, and express human emotions. It is an interdisciplinary field, spanning computer science, psychology, and cognitive science (Tao and Tan, 2005). Relevant studies usually extract feature patterns using techniques such as electroencephalogram (EEG) and electromyogram (EMG) for emotion recognition from physiological signals (Shen and Hu, 2019). Mental disorder may affect the brain under the influence of various biological, psychological, and social environmental factors, resulting in emotional, behavioral, and other mental activities, most of which are accompanied by either brain structure or functional lesions. Therefore, this study will apply affective computing to analyze the resting state brain network of patients with major depression (MDD) and schizophrenia (SCZ), and quantify their brain activity. Note that the comparison of the brain network with those of healthy people helps identify differences and assist in the medical diagnosis of mental disorders.

In this study, we selected functional near infrared spectroscopy (fNIRS) for the data collection from the prefrontal cortex (PFC) region. fNIRS is easy to operate, inexpensive, non-intrusive, and portable (Boas et al., 2004; Piper et al., 2014). The near infrared photons are weakly absorbed by biological tissues, and they can scatter across the brain surface (Villringer and Chance, 1997). Furthermore, during data acquisition, fNIRS is applicable to both clinical and laboratory studies, because the optical array does not harm for infants and children's brain. We selected PFC because many previous studies have demonstrated that PFC plays an important role in various high-level cognitive functions, such as executive functions (Miller and Cohen, 2001), decision-making (Wallis, 2007), reasoning and planning , social cognitive and moral judgment(Forbes and Grafman, 2010). It is possible to identify useful features for affective computing in this field.

Many studies examined resting state functional brain connectivity, using different experimental methods (Wang et al., 2018; Cai et al., 2018). Moreover, functional brain connectivity can be demonstrated by channel correlations. For example, pearson correlation analysis (CORR) gives the magnitude of temporal correlations, which may also occur between anatomically disjointed regions (Rubinov and Sporns, 2010). Beyond that, the correlation can be

⋆ This work was supported in part by the National Key Research and Development Program of China (Grant No.2019YFA0706200), in part by the National Natural Science Foundation of China (Grant No.61632014, No.61627808, No.61210010), in part by the National Basic Research Program of China (973 Program, Grant No.2014CB744600), in part by the Program of Beijing Municipal Science & Technology Commission (Grant No.Z171100000117005), and in part by the Fundamental Research Funds for the Central Universities (lzujbky-2020-66, lzujbky-2020-kb25, lzujbky-2020-kb08).

10.1016/j.ifacol.2021.04.195

analyzed in the frequency domain, by calculating the amplitude squared coherence coefficient (COH). Other studies use phase locking value (PLV) statistics to reflect connectivity. Intuitively, if the rise or fall in the fNIRS signal is larger than the baseline in both channels, the two channels are synchronous, or broadly speaking, they have high connectivity. Otherwise, if the rise or fall in the fNIRS signal is less than the baseline value, it indicates a lack of synchronization between the two channels, or generally speaking, a decrease in connectivity. In this study, we constructed brain networks as per these measurements.

The complexity of the brain network indicates that it has similarities with the network graph, and it has significant information transmission efficiency and local interconnectivity at the global level. A small-world network is a concept that has emerged from studying complex networks. If the average shortest path length between the two vertices of network is scaled with N as the maximum logarithm at a fixed average point, we consider it has a small-world property. This concept was first proposed by Duncan Watts and Steven Strogatz in 1998 (Watts and Strogatz, 1998). Moreover, small-world network model has multiple important parameters (Newman, 2001; Leung and Chau, 2007), (i) Clustering coefficient (C_p): the local efficiency in information network transfer; (ii) Characteristic path length (L_p): the global network efficiency and parallel information transmission ability (Latora and Marchiori, 2003); (iii) Normalized coefficient(γ/λ): normalization clustering coefficient/ normalized characteristic path length; (iv) Small-world parameters (σ): modular processing and efficient transmission of information between network characteristics modules; and (v) Global/Local efficiency ($E_{\text{glob}}/E_{\text{loc}}$): measures the ability of the network information transmission efficiency. By analyzing these features, this study shows the effect of mental disorders on the PFC network in the resting state, which may be a new approach of early warning and detecting mental problems via affective computing.

2. MATERIALS AND METHODS

2.1 Participants and Instrumentation

In this study, we recruited 35 MDD patients, 20 SCZ patients and 30 healthy control (HC) individuals from a psychiatric specialist hospital as participants. All of them were right-handed without color blindness, and at least had elementary education. A psychiatrist was responsible

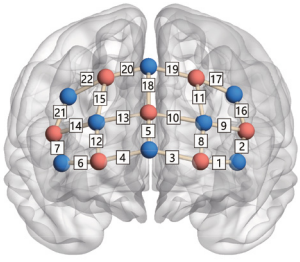

Fig. 1. The channel layout of the experiment (The blue dots represent the sources, the red dots represent the detectors, and the faint yellow lines represent the channels)

Table 1. The MNI coordinates of the channel layout

Channel Number	S - D	X(mm)	Y(mm)	Z(mm)
CH01	AF7 - Fp1	-33	59	-2
CH02	AF7 - F5	-47	46	6
CH03	Fpz - Fp1	-12	67	0
CH04	Fpz - Fp2	13	67	0
CH05	Fpz - AFz	1	64	14
CH06	AF8 - Fp2	34	59	-2
CH07	AF8 - F6	48	46	5
CH08	AF3 - Fp1	-24	63	9
CH09	AF3 - F5	-39	50	17
CH10	AF3 - AFz	-12	62	23
CH11	AF3 - F1	-23	52	32
CH12	AF4 - Fp2	25	63	9
CH13	AF4 - AFz	13	61	24
CH14	AF4 - F6	40	50	16
CH15	AF4 - F2	22	52	33
CH16	F3 - F5	-46	39	26
CH17	F3 - F1	-31	39	41
CH18	Fz - AFz	2	50	39
CH19	Fz - F1	-9	41	50
CH20	Fz - F2	10	41	50
CH21	F4 - F6	46	38	24
CH22	F4 - F2	30	40	41

for classifying them as either MDD, SCZ, or HC. Each of them was asked to fill out the Patient Health Questionnaire 15 item (PHQ-15), Generalized Anxiety Disorder 7 (GAD-7), Athens Insomnia Scale (AIS) and several other self-rating scales; moreover, they were required to sign informed consent documents before the experiments.

Herein, we present a 22-channel fNIRS device that uses eight dual wavelength light emitting diodes and seven electro-optical sensors. The sampling rate of the equipment is 7.8125Hz with two wavelengths: a long wavelength of 850nm and short wavelength of 760nm. The device was used to measure hemodynamic responses in the subjects' PFC. The channel layout is shown in Fig.1: the distance between each source and each detector is ∼3 cm. Table.1 lists the MNI coordinates corresponding to the channels.

2.2 Experiment Procedure and Data Acquisition

The experiment comprises a 5-min resting state. Before the experiment is initiated, detailed instructions are provided to the participant to ensure that he or she understands the process. The experimenter would then open the collecting device and snugly and stably place the optical fibers in the designated position. Turning on the device early aims to avoid the drift caused by itself. Moreover, sliding in the hair can cause signal attenuation. Although the PFC region has less hair compared to other parts of the scalpthe experimenter should always remove the hair and carefully place the fibers. In this study, participants will be informed to minimize unnecessary movements, close their eyes, and sit on a chair while remaining quiet. The whole experiment takes ∼15 min: Fig.2 shows the pipeline.

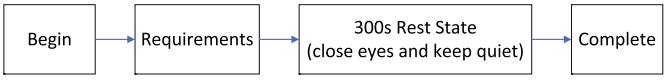

Fig. 2. The pipeline of the resting state experiment

2.3 Data Processing

Because of uncertain experimental factors, the motion artifacts of the fNIRS signals are produced by either unconscious cough or movement. This situation is particularly obvious in both the MDD and the SCZ groups. As per the calculation results of coefficient variation (CV) and direct observation of original data, 11 cases of data (5 from MDD, 3 from SCZ, and 3 from HC) were excluded; moreover, data from the remaining 74 participants were processed in the next steps.

(1) Intercept the data length to 270 s, with a uniform data length to stabilize the analysis;
(2) use the Homer2 toolbox to perform preprocessing (Huppert et al., 2006). obtain the optical density (OD) from the raw data by light intensity, and then the principle component analysis (PCA, 0.95) approach is applied to remove artifacts; and
(3) calculate blood oxygen concentration, obtain all HbO and HbR data of each participant, and then store as per the participant's type;

2.4 Correlation Analysis:

The following three types of correlation coefficients are calculated using the HbO and HbR data for each participant using built-in Matlab functions. Moreover, multiple 22 by 22 brain network connectivity matrices are obtained.

Pearson Correlation Coefficient (CORR) Describes the two time domain signals linear correlation relationship with values ranging from -1 to 1. If the two signals are completely negative correlation, the value is -1; however, if both signals have a completely positive correlation, the value is 1. Furthermore, if there is no linear correlation between the two signals, the value is 0.

Amplitude Squared Coherence Coefficient (COH) Describes the linear correlation between the two signals in the frequency domain, the values range from 0 to 1. At a certain frequency, if there is no correlation between these two signals, the value is 0, and the complete correlation is 1.

Phase Locking Value (PLV) Also referred to as the average phase coherent, it describes the relative phase difference between the two signals, which varies from 0 to 1. These two signals' phase difference is evenly distributed in the region of $-\pi$ to π, i.e., when there is no phase synchronization, the value is 0. However,when the phase difference is fixed from $-\pi$ to π within a fixed value, i.e, complete phase synchronization, the value is 1.

2.5 Network Analysis

For analyzing brain networks, we describe channels as nodes and functional connections between channels as the edges as per the graph theory. In all three groups, we use Gretna Toolbox (Rubinov and Sporns, 2010) to observe small-world properties and centrality.

Small-World For a graph G, where the number of nodes is N. The formula representation of these metrics can be identified as follows (Watts and Strogatz, 1998; Wang et al., 2015; Achard and Bullmore, 2007):

$$C_p = \frac{1}{N}\sum_{i\in G}\frac{E_i}{K_i\left(K_i-1\right)/2} \tag{1}$$

where E_i and K_i are the number of edges and nodes in subgraph Gi, respectively.

$$L_p = \frac{1}{N(N-1)}\sum_{i\neq j\in G} D_{\mathrm{ij}} \tag{2}$$

where D_{ij} is the shortest path length between the node i and node j.

$$E_{\mathrm{glob}} = \frac{1}{N(N-1)}\sum_{i\neq j\in G}\frac{1}{D_{\mathrm{ij}}} \tag{3}$$

where D_{ij} denotes the shortest path length between the node i and node j.

$$E_{\mathrm{loc}} = \frac{1}{N}\sum_{i\in G} E_{\mathrm{glob}}\,(\mathrm{i}) \tag{4}$$

where E_{glob} is the global efficiency of G_i, which is a subgraph of the neighbors of node i.

Small-world properties are defined as $\gamma = C_p^{\mathrm{net}}/C_p^{\mathrm{ran}} > 1$, $\lambda = L_p^{\mathrm{net}}/L_p^{\mathrm{ran}} \approx 1$, and $\sigma = \gamma/\lambda > 1$. Note that C_p^{net} and L_p^{net} are the C_p and L_p of real networks, respectively. Correspondingly, C_p^{ran} and L_p^{ran} are the C_p and L_p averages of 100 matched networks (with the same number of nodes, edges, and distributions as real brain networks). Moreover, E_{glob} quantifies the information exchanged by the entire network, while E_{loc} quantifies the network's resistance to a small number of failures. Note that C_p is inversely proportional to the E_{glob} for information transfer between network nodes using multiple parallel paths (Latora and Marchiori, 2003, 2001). Furthermore, E_{glob} is easier to estimate compared to C_p when we examine sparse networks; therefore, network efficiency can be used to quantify small-world property in a network.

Centrality Studying the centrality of the network is an approach to explore the structure of the network. The centrality of the channel is discussed in this study. Degree centrality is the most common and simplest approach to measure network centrality, measured by the degree of the node (the number of friends of users in the social network). Betweenness centrality is then obtained by the number of shortest paths between any two nodes in the network. If many of these shortest paths pass through a node, the node is considered to have high mediation centrality (Freeman, 1977).

3. RESULTS AND ANALYSIS

3.1 Correlation Coefficients

We performed a statistical analysis of the correlation coefficient matrices and calculated their mean value (mean) and standard deviation (SD), which are shown in Table.2. Furthermore, they are normally distributed as confirmed by the Q-Q graph. Because the correlation coefficient matrix is symmetric along the diagonal, we extract the

Table 2. Mean value and standard deviation of correlation coefficients

Group (mean ± SD)	CORR		COH		PLV	
	HbO**	HbR	HbO**	HbR*	HbO**	HbR
HC	0.74 ± 0.077	0.43 ± 0.128	0.68 ± 0.080	0.42 ± 0.081	0.67 ± 0.073	0.45 ± 0.085
MDD	0.74 ± 0.085	0.44 ± 0.131	0.68 ± 0.084	0.40 ± 0.084	0.67 ± 0.080	0.47 ± 0.089
SCZ	0.78 ± 0.070	0.43 ± 0.144	0.72 ± 0.069	0.42 ± 0.082	0.73 ± 0.062	0.47 ± 0.093

* p <0.01, ** p <0.001

correlation coefficients from the lower half of the triangle for one-way ANOVA analysis and post-hoc test. The results of the group comparison demonstrate that, except for CORR and PLV calculated by HbR, the other four groups are statistically significant ($p < 0.01$). Moreover, multiple comparisons of the four groups of data demonstrate that SCZ is significantly different from the other two groups ($p < 0.001$) for CORR, COH and PLV calculated by HbO; however, MDD is significantly different from the other two groups ($p < 0.05$) for the COH calculated by HbR.

Furthermore, we performed a t-test on the three types of correlation coefficients for pairwise comparison. Because the two sample t-test requires samples with the same dimension, we randomly selected 17 samples from HC and MDD. The results of the t-test can be observed in the matrices in Fig.3. Channels showing significant differences ($p < 0.05$) are marked with dark colors in the third column. To summarize, both MDD and SCZ show little difference, while HC shows considerable difference with the other two groups. Consistent with the previous one-way ANOVA analysis, the difference between HC and SCZ is obvious

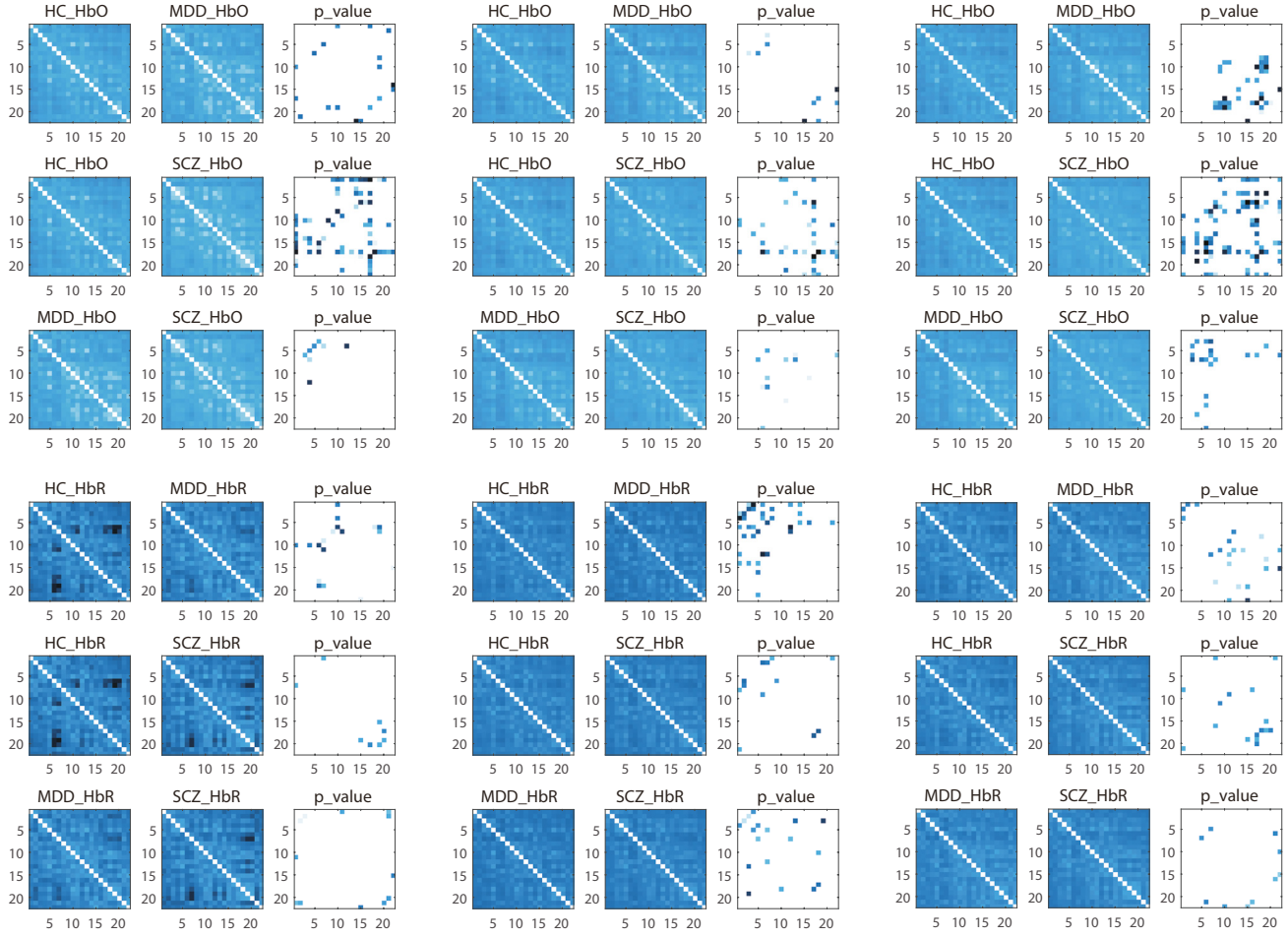

Fig. 3. T-test results of connection matrices (The left two columns of each subgraph are the correlation coefficient matrices on average for each group. Moreover, the right column shows the t-test results, and the dark squares indicate that the two channels corresponding to this point are significantly different between different groups ($p < 0.05$). The three rows above are calculated from the HbO data, and the three rows below are calculated from the HbR data. The three rows are HC and MDD, HC and SCZ, and MDD and SCZ for comparison, where (a) is calculated by CORR; (b) is calculated by COH; (c) is calculated by PLV)

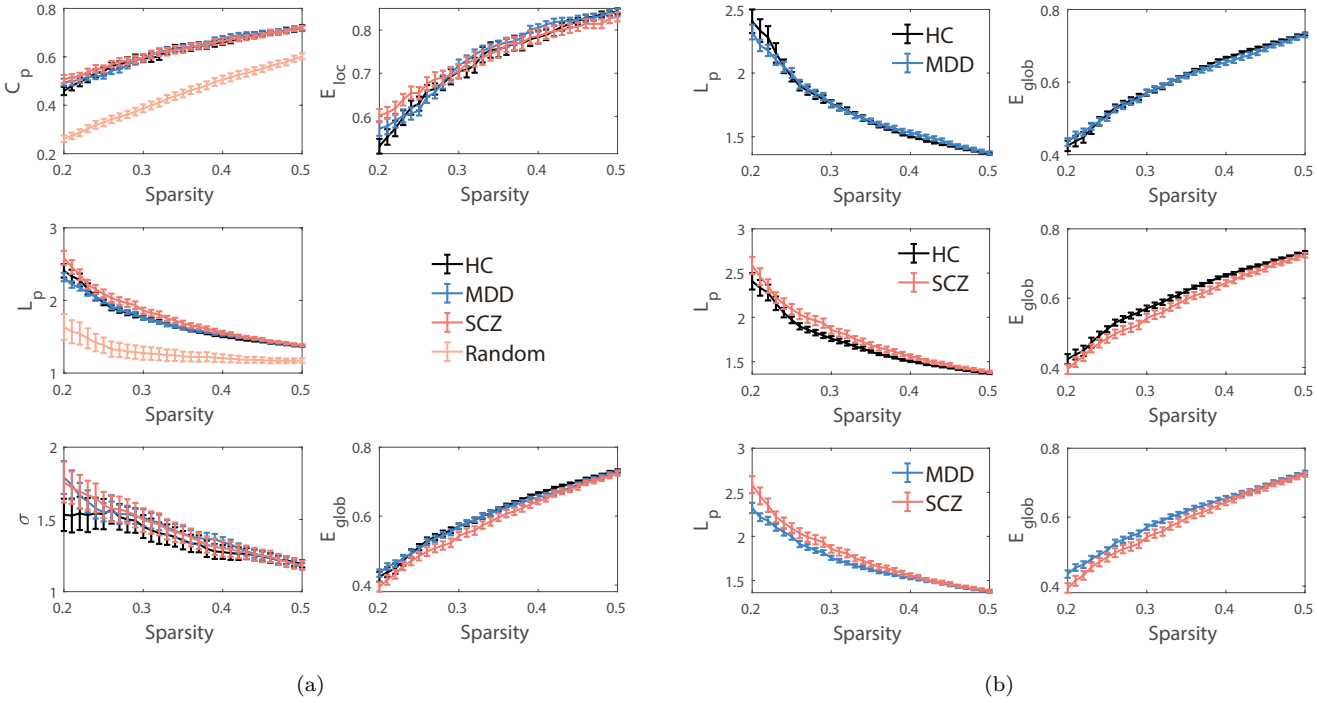

Fig. 4. The small-world properties and the network efficiency in a range of sparsity thresholds (20%-50%, 1% intervals). ((a) The small-world properties and the network efficiency of the real network and matched random network. The left three figures are the clustering coefficient (C_p), characteristic path length (L_p), and small-world parameters (σ), whereas the right two figures are global efficiency (E_{glob}) and local efficiency (E_{loc}). (b) The paired comparison of different groups on characteristic path length (L_p) and global efficiency (E_{glob})) low sparsity threshold region. This may indicate that SCZ has a low global efficiency under a small sparsity threshold than the other two groups

in all correlation coefficients calculated by HbO; however, that between HC and MDD is more obvious in COH calculated by HbR.

3.2 Small-world Properties

Three groups have small-world properties as the delta parameter is > 1 at all sparsity thresholds (20%-50%, 1% intervals). Fig.4(a) shows the small-world properties of the real network and the C_p and L_p of the matched random network. Note that both C_p and L_p of the real brain network are significantly higher than a random network.

As shown in Fig.4(a), L_p and E_{glob} of SCZ are significantly different from the other two groups when the sparsity is between 0.25 and 0.4. Therefore, for additional verification, L_p and E_{glob} are extracted and drafted in Fig.4(b). For HC and SCZ, the L_p of SCZ is significantly higher than that of HC between 0.25 and 0.42; however, the E_{glob} of SCZ is significantly lower than that of HC between 0.25 and 0.44, which conforms to the reciprocal relationship between L_p and E_{glob} in the formulaic definition. Note that similar differences are observed between MDD and SCZ, but are not as obvious as both HC and SCZ; however, they show significant differences in the low sparsity threshold region.

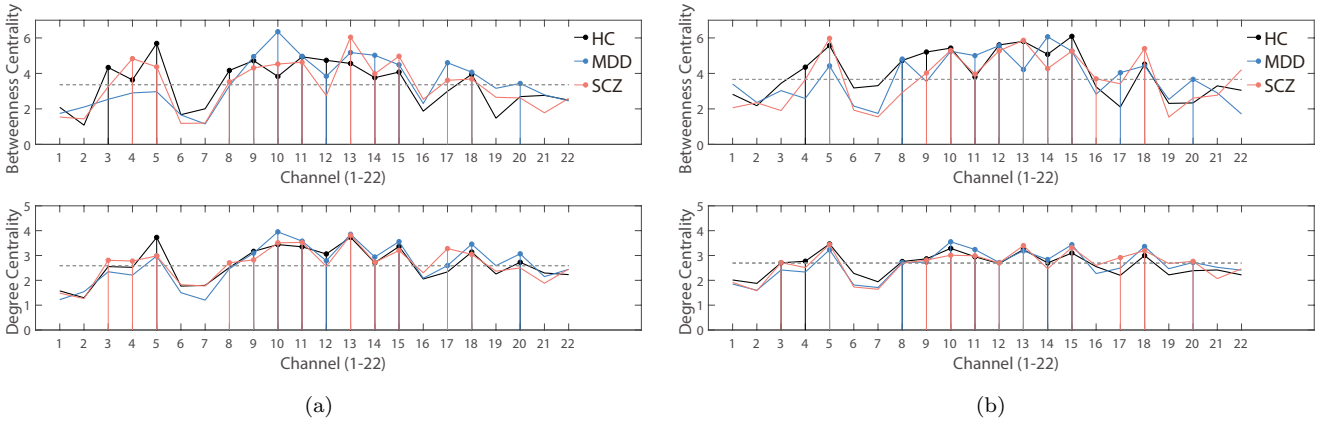

Fig. 5. Degree centrality and betweenness centrality of three groups. (The dotted line marks the median of the centrality value: (a)calculated by HbO data and (b)calculated by HbR data)

This may indicate that MDD has a high global efficiency under small sparsity threshold than other two groups.

3.3 Centrality

Fig.5 shows the degree centrality and betweenness centrality of all 22 channels. Degree centricity shows good consistency in both HbO and HbR data of three groups. There is a higher value concentrate upon channel 5,10,13,15, and 18 (nodes). With the channel layout, these channels are located in the middle of the network, which is consistent with the actual situation. However, the intensity of betweenness centrality on the various channels is somewhat mixed, because these three groups of data show significant differences for certain channels. Some studies have demonstrated similar results (Sun et al., 2019). Therefore, betweenness centrality can also be used as an indicator of affective computing to evaluate the effects of mental disorders on PFC regions.

4. CONCLUSION

In this study, we used the fNIRS method to collect the resting state data of MDD, SCZ, and HC for the PFC region. The correlation of three datasets was calculated from the time domain, frequency domain, and phase domain. Moreover, based on correlation coefficient matrices, small-world model parameters such as C_p, L_p and other network model parameters such as degree centrality and betweenness centrality is calculated. The results suggest that mental disorders damage the local connectivity of the functional brain networks of patients, which is consistent with the results of earlier studies (Li et al., 2017). Moreover, we predicted that the fNIRS method will be used to design a portable machine to participate in the predictive or detection of mental disorders. In the following study, based on what we have performed, a task-state experiment can be designed to further explore the impact of mental disorders on brain functional networks and to identify additional effective and reliable methods of affective computing.

REFERENCES

Achard, S. and Bullmore, E. (2007). Efficiency and cost of economical brain functional networks. *PLoS Comput Biol*, 3(2), e17.

Boas, D.A., Dale, A.M., and Franceschini, M.A. (2004). Diffuse optical imaging of brain activation: approaches to optimizing image sensitivity, resolution, and accuracy. *Neuroimage*, 23, S275–S288.

Cai, L., Dong, Q., and Niu, H. (2018). The development of functional network organization in early childhood and early adolescence: A resting-state fnirs study. *Developmental cognitive neuroscience*, 30, 223–235.

Forbes, C.E. and Grafman, J. (2010). The role of the human prefrontal cortex in social cognition and moral judgment. *Annual review of neuroscience*, 33, 299–324.

Freeman, L.C. (1977). A set of measures of centrality based on betweenness. *Sociometry*, 40(1), 35–41.

Huppert, T.J., Hoge, R.D., Diamond, S.G., Franceschini, M.A., and Boas, D.A. (2006). A temporal comparison of bold, asl, and nirs hemodynamic responses to motor stimuli in adult humans. *Neuroimage*, 29(2), 368–382.

Latora, V. and Marchiori, M. (2001). Efficient behavior of small-world networks. *Physical review letters*, 87(19), 198701.

Latora, V. and Marchiori, M. (2003). Economic small-world behavior in weighted networks. *The European Physical Journal B-Condensed Matter and Complex Systems*, 32(2), 249–263.

Leung, C. and Chau, H. (2007). Weighted assortative and disassortative networks model. *Physica A: Statistical Mechanics and its Applications*, 378(2), 591–602.

Li, X., Zhuang, J., Hu, B., Jing, Z., Ning, Z., Mi, L., Ding, Z., Jing, Y., Lan, Z., and Lei, F. (2017). A resting-state brain functional network study in mdd based on minimum spanning tree analysis and the hierarchical clustering. *Complexity*, 2017, 1–11.

Miller, E.K. and Cohen, J.D. (2001). An integrative theory of prefrontal cortex function. *Annual review of neuroscience*, 24(1), 167–202.

Newman, M.E. (2001). Scientific collaboration networks. ii. shortest paths, weighted networks, and centrality. *Physical review E*, 64(1), 016132.

Piper, S.K., Krueger, A., Koch, S.P., Mehnert, J., Habermehl, C., Steinbrink, J., Obrig, H., and Schmitz, C.H. (2014). A wearable multi-channel fnirs system for brain imaging in freely moving subjects. *Neuroimage*, 85, 64–71.

Rubinov, M. and Sporns, O. (2010). Complex network measures of brain connectivity: uses and interpretations. *Neuroimage*, 52(3), 1059–1069.

Shen, J. and Hu, B. (2019). An improved empirical mode decomposition of electroencephalogram signals for depression detection. *IEEE Transactions on Affective Computing*, PP(99).

Sun, S., Li, X., Zhu, J., Wang, Y., La, R., Zhang, X., Wei, L., and Hu, B. (2019). Graph theory analysis of functional connectivity in major depression disorder with high-density resting state eeg data. *IEEE Transactions on Neural Systems and Rehabilitation Engineering*, 27(3), 429–439.

Tao, J. and Tan, T. (2005). Affective computing: a review. *affective computing and intelligent interaction*, 3784, 981–995.

Villringer, A. and Chance, B. (1997). Non-invasive optical spectroscopy and imaging of human brain function. *Trends in neurosciences*, 20(10), 435–442.

Wallis, J.D. (2007). Orbitofrontal cortex and its contribution to decision-making. *Annu. Rev. Neurosci.*, 30, 31–56.

Wang, J., Wang, X., Xia, M., Liao, X., Evans, A., and He, Y. (2015). Gretna: a graph theoretical network analysis toolbox for imaging connectomics. *Frontiers in human neuroscience*, 9, 386.

Wang, M.Y., Zhang, J., Lu, F.M., Xiang, Y.T., and Yuan, Z. (2018). Neuroticism and conscientiousness respectively positively and negatively correlated with the network characteristic path length in dorsal lateral prefrontal cortex: A resting-state fnirs study. *Brain and behavior*, 8(9), e01074.

Watts, D.J. and Strogatz, S.H. (1998). Collective dynamics of small-worldnetworks. *nature*, 393(6684), 440.